Airway epithelial wounds in rhesus monkey generate ionic currents that guide cell migration to promote healing

Yao-Hui Sun, Brian Reid, Justin H. Fontaine, Lisa A. Miller, Dallas M. Hyde, Alex Mogilner and Min Zhao

You might find this additional info useful...

This article cites 61 articles, 18 of which you can access for free at:
http://jap.physiology.org/content/111/4/1031.full#ref-list-1

This article has been cited by 1 other HighWire-hosted articles:
http://jap.physiology.org/content/111/4/1031#cited-by

Updated information and services including high resolution figures, can be found at:
http://jap.physiology.org/content/111/4/1031.full

Additional material and information about *Journal of Applied Physiology* can be found at:
http://www.the-aps.org/publications/jappl

This information is current as of September 6, 2013.

Airway epithelial wounds in rhesus monkey generate ionic currents that guide cell migration to promote healing

Yao-Hui Sun,[1] Brian Reid,[1] Justin H. Fontaine,[2] Lisa A. Miller,[2] Dallas M. Hyde,[2] Alex Mogilner,[3] and Min Zhao[1,4]

[1]*Department of Dermatology, School of Medicine;* [2]*Department of Anatomy, Physiology and Cell Biology, School of Veterinary Medicine, and California National Primate Research Center;* [3]*Department of Neurobiology, Physiology and Behavior, and Department of Mathematics, University of California, Davis; and* [4]*Department of Ophthalmology, School of Medicine, University of California, Davis, Sacramento, California*

Sun YH, Reid B, Fontaine JH, Miller LA, Hyde DM, Mogilner A, Zhao M. Airway epithelial wounds in rhesus monkey generate ionic currents that guide cell migration to promote healing. *J Appl Physiol* 111: 1031–1041, 2011. First published June 30, 2011; doi:10.1152/japplphysiol.00915.2010.—Damage to the respiratory epithelium is one of the most critical steps to many life-threatening diseases, such as acute respiratory distress syndrome and chronic obstructive pulmonary disease. The mechanisms underlying repair of the damaged epithelium have not yet been fully elucidated. Here we provide experimental evidence suggesting a novel mechanism for wound repair: endogenous electric currents. It is known that the airway epithelium maintains a voltage difference referred to as the transepithelial potential. Using a noninvasive vibrating probe, we demonstrate that wounds in the epithelium of trachea from rhesus monkeys generate significant outward electric currents. A small slit wound produced an outward current (1.59 μA/cm^2), which could be enhanced (nearly doubled) by the ion transport stimulator aminophylline. In addition, inhibiting cystic fibrosis transmembrane conductance regulator (CFTR) with CFTR(Inh)-172 significantly reduced wound currents (0.17 μA/cm^2), implicating an important role of ion transporters in wound induced electric potentials. Time-lapse video microscopy showed that applied electric fields (EFs) induced robust directional migration of primary tracheobronchial epithelial cells from rhesus monkeys, towards the cathode, with a threshold of <23 mV/mm. Reversal of the field polarity induced cell migration towards the new cathode. We further demonstrate that application of an EF promoted wound healing in a monolayer wound healing assay. Our results suggest that endogenous electric currents at sites of tracheal epithelial injury may direct cell migration, which could benefit restitution of damaged airway mucosa. Manipulation of ion transport may lead to novel therapeutic approaches to repair damaged respiratory epithelium.

transepithelial potential; electric fields; wound healing; cystic fibrosis transmembrane conductance regulator

THE AIRWAY EPITHELIUM FORMS the front line in respiratory and pulmonary defense against inhaled substances including pathogens and airborne allergens and therefore actively contributes to the innate immune system. The airway epithelium provides a barrier against physical, chemical, and biological insult through clearance of the mucus, transport of ions and water, and sealing of the paracellular routes by tight junctions (11). The epithelial lining is often compromised in diseases such as chronic obstructive pulmonary disease (14, 15, 19, 36) and acute respiratory distress syndrome (22, 54). Epithelial damage may in part be a consequence of ongoing inflammation or mechanical stress caused by bronchoconstriction but may also reflect host-compromising susceptibility factors (48). Efficient repair of the airway epithelial barrier is therefore critical to maintaining respiratory function.

Healing of damaged airway epithelium comprises a cascade of tightly regulated events. The initial response involves migration and spreading of neighboring epithelial cells to cover the denuded surface, followed by migration and proliferation of localized progenitor cells to restore cell numbers, as well as differentiation to restore epithelial functions (47, 57). Many factors may contribute to airway epithelial migration. Following damage, epithelial cells at wounds become migratory in response to chemokines, colony-stimulating factors, and growth factors including EGF, TGF-β, and other factors released at wounds. These biochemical factors stimulate and guide cell migration (7, 36). Failure or delay of repair to the airway epithelium may result in microbial colonization and overactivation of the immune system. This may lead to a massive inflammatory response that can become pathological, or even fatal in susceptible individuals, yet no effective therapeutic approaches are currently available to directly stimulate the reparative response.

Electric fields (EFs) direct cell migration and promote epithelial wound healing in the cornea and skin. The transepithelial potential difference (TEP) is an intrinsic property of polarized epithelia with ion transporting capacity. When injury damages the epithelium, the TEP collapses at the wound resulting in laterally oriented EFs with the cathode at the wound center (5, 26, 31, 38, 39). Damage to rat cornea, for example, generates an outward electric current that lasts for an hour at a peak of 10 μA/cm^2 (39). Similar electric currents are detected at human skin wounds (26, 31, 61). Keratinocytes and corneal epithelial cells respond to EFs of 40 to 180 mV/mm and migrate towards the cathode, a phenomenon termed electrotaxis or galvanotaxis. Field strengths that are required to induce electrotaxis are within the range of naturally occurring EFs found at skin and corneal wounds (28, 44, 59–61). Although endogenous wound currents were first recorded over 150 years ago, their significance has remained poorly understood and largely ignored (24, 58). However, the existence of these endogenous wound currents/EFs has been confirmed by modern techniques such as glass microelectrodes, vibrating probes, microneedle arrays, and bioelectric imagers (3–5, 13, 18, 26, 31, 39, 53). There is a growing body of evidence that suggests an important role for endogenous EFs in wound

---

Address for reprint requests and other correspondence: M. Zhao, Dermatology & Ophthalmology Research, Institute for Regenerative Cures, Univ. of California at Davis CA, School of Medicine, 2921 Stockton Blvd., Rm. 1617, Sacramento, CA 95817 (e-mail: minzhao@ucdavis.edu).

healing (20, 24, 29, 30, 32, 41, 58). More recently, we and others (17, 58, 61) provided experimental evidence suggesting that EFs may serve as a powerful guidance signal to direct cell migration in wound healing, overriding other well-accepted cues, such as mechanical forces, chemical signals, and contact inhibition.

Respiratory epithelia also generate and maintain a significant TEP (27, 50). We hypothesize that injury to the respiratory epithelium short circuits the TEP and generates laterally oriented wound EFs, which can stimulate and direct migration of airway epithelial cells in wound healing. We tested this hypothesis with cells and tissues from a nonhuman primate, the rhesus monkey (*Macaca mulatta*), which is genetically and evolutionarily closer to humans than any other mammalian species and therefore provides the best animal model to study asthma and other respiratory diseases. Its immune system is comparable to that of humans (35). In the context of the respiratory system, it displays very similar cell types and epithelial structure to humans (34). Moreover, the cellular biology and bioelectric properties of the airway epithelia of both species are highly conserved (21).

We report that *1*) epithelial wounds in trachea from rhesus monkeys generate electric currents; *2*) manipulation of the ion transport regulator cystic fibrosis transmembrane conductance regulator (CFTR) significantly affects wound electric currents; *3*) tracheobronchial epithelial cells respond to a small applied EF by enhanced directional migration towards the cathode; and *4*) an applied EF promotes wound healing in vitro. These results suggest a new mechanism in airway epithelial wound healing and introduce the possibility of using pharmacological manipulation of ion transport to modulate airway epithelial repair.

MATERIALS AND METHODS

Wounding of the tracheal epithelium and measurement of electric current. Trachea, along with mainstem bronchi, from adult rhesus macaque monkeys (*Macaca mulatta*), were obtained from the California National Primate Research Center and brought to our laboratory within 30 min of collection. The use of necropsy samples was approved by the University of California, Davis, Institutional Animal Use and Care Committee. The trachea was cleaned by removing excess connective tissue and blood vessels and flushed several times with minimal essential medium (SMEM; Fisher) plus antibiotics. A cylindrical section (~1.5 cm in length) was sectioned and cut to give two hemi-cylindrical pieces (Fig. 1A). A small slit epithelial wound was made with a scalpel fitted with a #11 blade under a dissecting microscope (Olympus SV40). Electric currents were measured before and after wounding using a vibrating probe. These two measurements were not made continuously, as we had to stop in between to make the wound. However, the interrupted time was kept as short as possible. In most cases it was <5 min.

The vibrating probe technique has been described in detail previously (38). Briefly, an insulated stainless steel electrode, electroplated with gold and platinum, was vibrated at high frequency in solution far away (~2 cm) from the specimen to establish a baseline. This was the reference position. Under the dissecting microscope, the probe that was mounted on a three-dimensional micromanipulator was then moved to measurement position, ~50 μm above the center of the wound (Fig. 1A). As the probe vibrates, the charge at the electrode tip oscillates in proportion to the size of the electric current. As soon as the trace becomes steady with no further increase, the probe is moved slowly back to its reference position while the trace falls down to baseline (Fig. 1C). Measurements were done in medium used for
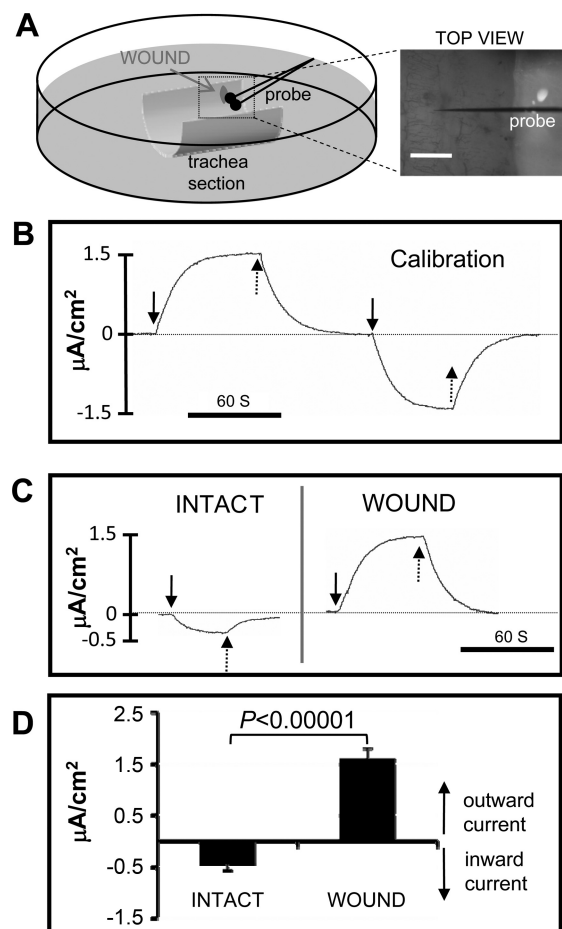

Fig. 1. Wounds in trachea generate electric currents. *A*: schematic showing a hemi-cylindrical section of trachea mounted in a plastic 35-mm Petri dish containing BEGM culture medium. Trachea wound and vibrating probe were viewed under a dissection microscope (TOP VIEW, *right*). Scale bar = 0.5 mm. *B*: vibrating probe was calibrated in BEGM medium. After establishing a stable baseline (dashed line at 0), a current of 1.5 μA/cm² was applied, first in one direction and then in the opposite direction. Solid arrows show when the current was switched on, and dashed arrows show when the current was switched off. Scale bar = 60 s. *C*: typical electric currents recorded from an intact and then wounded (wound was made immediately before the recording, <5 min prior) tracheal epithelium. Solid arrows show when the probe was brought to the measuring point, and dashed arrows show when it was brought away from the measuring point to the reference position. Inward/outward currents are below/above the baseline (dashed line at 0) respectively. Scale bar = 60 s. *D*: intact tracheal epithelium showed small inward currents. Small slit wounds had larger outward currents (*P* < 0.00001; *n* = 9).

culture of tracheobronchial epithelial cells (see *Culture of monkey tracheobronchial epithelial cells*) at room temperature. All measurements were done at room temperature within 1 h of trachea removal from necropsy. The probe was calibrated at the start and end of each experiment in a known current from a constant current calibrator unit (Fig. 1B).

To measure tracheal epithelial wound current modulated by pharmacological agents, aminophylline (10 mM) or CFTR(Inh)-172 (10 μM) was added to the medium as previously described (9, 39, 46). Tissues were exposed to the drug for 20 min before measurement. Both drugs were purchased from Sigma-Aldrich. The 100× stock solutions were made in DMSO according to the manufacturer's instructions and stored at −20°C until use.

Culture of monkey tracheobronchial epithelial cells. Tracheobronchial epithelial cells were isolated as previously described (1). Cleaned trachea (see *Wounding of the tracheal epithelium and mea-*

surement of electric current) was digested overnight at 4°C in SMEM medium plus 0.1% protease (Type XIV; Sigma-Aldrich). Further digestion was halted by addition of 10% FBS. Primary monkey tracheobronchial epithelial cells were flushed off and collected by centrifugation at 300 g for 5 min. After one wash with SMEM plus 10% FBS, cells were resuspended in bronchial epithelial cell growth medium with growth supplements (BEGM; BulletKit; Lonza) plus 2% FBS and cultured in T25 flasks coated with FNC (fibronectin and collagen) coating mix (Athena Enzyme Systems) at 37°C in a humidified CO_2 (5%) incubator. Medium was replaced by BEGM plus 1% FBS the next day and then changed every 2–3 days with serum-free BEGM. These protocols and special media support tracheobronchial epithelial cell growth (16).

Applying the direct current EF. The electrotaxis experiments were carried out as previously described (45, 59). Primary tracheobronchial epithelial cells were detached from the tissue culture flask by trypsinization with 0.05% typsin/0.53 mM EDTA (Invitrogen). Upon detachment, an equal volume of trypsin neutralization solution (Fisher) was added to halt further digestion. Cells were collected by centrifugation, washed once with BEGM, and seeded in electrotactic chambers (10 × 10 × 0.1 mm) built over 48 × 60 mm² #1 cover glasses that were coated with FNC coating mix. After 4 h of incubation, unattached cells were removed by being washed with BEGM. These custom-made electrotactic chambers with small cross-sectional area provided high resistance to current flow and minimized Joule heating during EF application. To eliminate toxic products from the electrodes that might be harmful to cells, salt bridges made with 1% agar gel in Steinberg's solution [58 mM NaCl, 0.67 mM KCl, 0.44 mM $Ca(NO_3)_2$, 1.3 mM $MgSO_4$, and 4.6 mM Trizma base pH 7.8–8.0] were used to connect silver/silver chloride electrodes in beakers of Steinberg's solution to pools of excess BEGM at either end of the electrotactic chamber.

Microscopy and time-lapse imaging. We confirmed the cultured cells as tracheobronchial epithelial cells by visualization of cilia. Cells were fixed in 3.7% paraformaldehyde and observed with an Olympus CX71 microscope by using a ×40 oil lens. To record ciliary beating, live tracheobronchial epithelial cells were localized with a phase contrast microscope. Video streams were acquired using the Meta-Morph image system 7.5 (Molecular Devices) and an Electron Multiplier CCD camera (ImagEM; Hamamatsu).

Cell migration was recorded with a Zeiss AxioVert 40 Microscope with a Hamamatsu CCD digital camera (Hamamatsu) attached. Time-lapse images were recorded using a SimplePCI 5.3 imaging system with a motorized X, Y, Z stage (BioPoint 2, Ludl Electronic Products). Typically in each experiment, six to eight fields under a ×10 low-power objective were chosen. Images were taken at 2- or 5-min intervals depending on the purpose of each experiment. The temperature was maintained within a 37°C incubation chamber (Solent Scientific) during each experiment.

Quantification of cell migration. Time-lapse images were imported into ImageJ. Tracks were marked using the MtrackJ tool and plotted using the Chemotaxis tool. Three parameters of cell migration were quantified. *1*) Directedness: a measurement quantifying how directionally cells migrated in response to an EF (49). The angle that each cell moved along with respect to the EF vector was measured, and its cosine value was calculated and used as a directedness value (12). If a cell moves perfectly along the field vector towards the cathode or the right in the case of no EF controls, the cosine of this angle is 1; if a cell moves perpendicularly to the field vector or to the *x*-axis in the case of no EF controls, the cosine of this angle is 0; and if a cell moves directly towards the anode or the left in the case of no EF controls, the cosine of this angle is −1. *2*) Trajectory velocity: the trajectory distance (μm) traveled by the cell divided by the time. *3*) Displacement speed: the straight line distance (μm) between the start and end points divided by the time.

Cells were chosen by following these criteria. *1*) Only live cells with good shape and light reflection were included for analysis. Dead cells that did not move were excluded. *2*) Cells interfering with the migration of each other were excluded. *3*) Cells had to be visible during the whole recording period (90–150 min). At least 50 cells were counted in each experiment.

Wound healing assay. The epithelial wound closure assay was performed as previously described (42). The tracheobronchial epithelial cells were grown to confluence in custom-made electrotactic chambers built on #1 cover glasses coated with FNC coating mix. Linear wounds ~0.2 mm in width were scraped with a standard 200-μl pipette tip. The wounded monolayer was rinsed with BEGM to remove cellular debris. To assay the effect of an EF on wound healing in vitro, an EF of 200 mV/mm was applied perpendicularly to the scratch wound, with no EF as a control. Three fields of each wound were recorded under a ×10 objective as above (see *Microscopy and time-lapse imaging* for details) at 5-min intervals in a 37°C incubation chamber (Solent Scientific) for 5 h. HEPES (25 mM) was added to the culture medium to stabilize pH during the experiments (45). Care was taken to avoid contamination throughout each experiment.

Wound areas were measured using ImageJ software and plotted as "remaining wound area" (percentage of the initial wound area). In the cases of applied EFs, the migration speeds of wound edges advancing towards to the cathode were calculated and treated as a collective migration speed. Significance was drawn by comparison with the migration speeds of wound edges under no EF conditions.

Statistics. All experiments were repeated at least three times. In most cases a representative experiment is shown, unless stated otherwise. Data are presented as means ± SE. Differences between groups were analysed using the paired or unpaired two-tailed Student's *t*-test. A *P* value of <0.05 is considered as significant.

RESULTS

Tracheal epithelial wounds produce outward electric currents that can be manipulated by an ion transport enhancer/inhibitor. We first determined electric currents at epithelial wounds in rhesus monkey trachea using the noninvasive vibrating probe. These measurements were done in the presence of BEGM medium. As exemplified in Fig. 1*C*, intact epithelium in excised trachea maintained small inward currents (defined as the flow of positive charge) of −0.46 ± 0.1 μA/cm² (Fig. 1*D*). Immediately after a slit wound was made, large outward currents (Fig. 1*C*) of 1.59 ± 0.21 μA/cm² were detected, which is statistically greater than that found in unwounded epithelium (*P* < 0.00001; Fig. 1*D*). This electric current results from a combination of net outward flow of cations and inward flow of anions. An equal and opposite current must flow within the epithelium and underlying tissues to generate an intra-tissue field with the negative pole at the wound site.

To confirm that the electric currents at wounds were not merely passive leakage but instead were due to active transport of ions, we used pharmacological agents to test whether the currents could be regulated. Aminophylline is a competitive nonspecific phosphodiesterase inhibitor that raises intracellular cAMP levels and enhances net Cl^- efflux in corneal epithelium (from aqueous to tear side; Ref. 56). Using cornea as a model, we found that the Cl^- efflux was enhanced in the intact epithelium by aminophylline treatment. Cl^- ions then flow back into the wound site forming a loop of Cl^- flux. Treatment with aminophylline enhances the Cl^- efflux, thus driving more Cl^- flux back into the wound site and increasing the outward current at the wound (52). In the context of ion transport, we reasoned that this may also be applicable to respiratory epithe-

lium based on their functional similarity. As expected, aminophylline treatment (10 mM) nearly doubled the outward current size to 3.2 ± 0.49 μA/cm², significantly greater than that of control wounds ($P < 0.01$; Fig. 2), in respiratory epithelium.

CFTR is a cAMP-regulated Cl⁻ channel localized in the apical membrane of epithelial cells (6). In addition to its primary function of Cl⁻ transport, CFTR is also permeable to HCO_3^- and regulates Na⁺ transportation (40). Pretreatment with CFTR(Inh)-172 (10 μM), a CFTR inhibitor, for 20 min, significantly reduced the outward currents at tracheal epithelial wounds (0.17 ± 0.03 μA/cm²; $P < 0.001$; Fig. 2). Interestingly, neither aminophylline nor CFTR(Inh)-172 had any significant effect on the resting currents at intact tracheal epithelium. Although treatment with aminophyline increased the inward electric currents slightly, the change was statistically insignificant [CFTR(Inh)-172, $P > 0.4$; aminophylline, $P > 0.09$; Fig. 2B]. These results suggest that the wound current is a regulated ion transport process, instead of mere leakage due to injury.

Applied EFs direct migration of tracheobronchial epithelial cells towards the cathode. We then tested whether primary cultures of tracheobronchial epithelial cells respond to applied EFs. We first confirmed some features of tracheobronchial epithelial cells. Clear cilia on the surface of paraformaldehyde-fixed tracheobronchial epithelial cells could be observed (data not shown). Further confirmation with high speed time-lapse recording under higher magnification (×400) showed ciliary beating (data not shown).
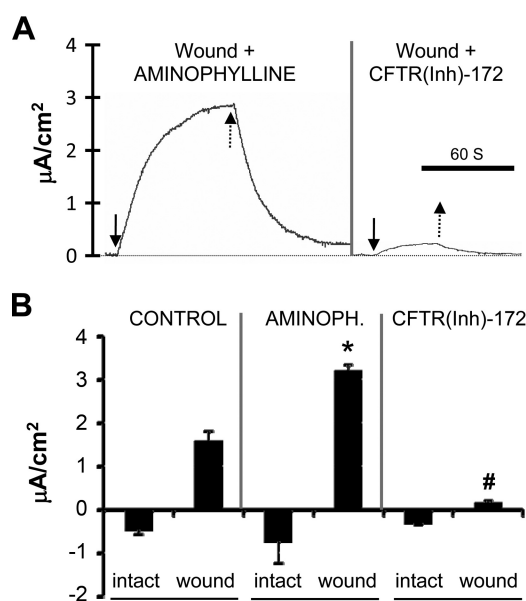

Fig. 2. Pharmacological manipulation of ion transport significantly affects wound electric currents. *A*: typical electric currents recorded from different tracheal epithelial wounds (wounds were made immediately before the recording, <5 min prior) in the presence of pharmacological drugs. Solid arrows show when the probe was moved to the wound, and dashed arrows show the probe moving away from the wound. Scale bar = 60 s. *B*: aminophylline doubled wound currents compared with control (*$P < 0.01$; $n = 7$) while cystic fibrosis transmembrane conductance regulator (CFTR) inhibitor CFTR(Inh)-172 significantly reduced wound currents (#$P < 0.0001$; $n = 6$). There was no significant difference between the unwounded measurements ($P > 0.09$).

Secondly, we exposed the cells to an applied EF. Tracheo-bronchial epithelial cells showed robust directional migration towards the cathode in an EF of 50 mV/mm (Fig. 3A, *left*). Cells cultured under the same conditions without an applied EF migrated in random directions (Fig. 3A, *right*). Lines in Fig. 3A show trajectories of cell migrations during a 60-min time course. With the position of all cells at time zero placed at the origin, the trajectories showed a random distribution in no EF controls (the mean directedness value was −0.058 ± 0.093, Fig. 3C and Supplemental File S1; Supplemental Material for this article is available online at the *J Appl Physiol* website), while those in an EF showed directed migration towards the cathode (Fig. 3B and Supplemental File S2). In an EF of 50 mV/mm, 89 out of 104 cells (85.58%) migrated towards the cathode during a time course of 145 min. The remaining 15 cells (14.42%, highlighted in gray) migrated towards the anode (*right*) with very short migratory distances (the mean directedness value was 0.701 ± 0.045; Fig. 3B). The majority of cells appeared to respond to the applied field within minutes. In the control culture without an EF, 58 out of 110 cells (52.73%) migrated towards the left while 52 (47.27%) migrated towards the right (the mean directedness value was 0.035 ± 0.071; Fig. 3C).

Switching EF polarity reverses the migratory direction of tracheobronchial epithelial cells. We further tested whether reversal of the field polarity reverses the migratory direction of tracheobronchial cells. Similar to other epithelial cells (28, 60), the tracheal epithelial cells reversed their direction of migration when EF polarity was reversed. As the EF strength changed the reversal responses varied. In general, for the cathode-directed migratory cells, two types of reversal responses were observed. Figure 4A shows time-lapse photographs from a representative experiment in which the cells were exposed to an EF of 50 mV/mm for 100 min and then the field polarity was reversed for 80 min. One cell reversed immediately (i.e., Fig. 4A, *cell 6*), while some other cells (e.g., Fig. 4A, *cells 1 to 4*) made a U-turn that took 10 to 20 min (Supplemental File S3). By using MtrackJ software, we were able to track the trajectories of migratory cells following a switch in EF polarity. In a particular assay of a 240-min time course (EF = 50 mV/mm, $n = 52$), during the first half of the experiment, 46 (88.46%) cells migrated towards the cathode (Fig. 4B, the mean directedness value was 0.705 ± 0.059). Following the reversal of the field polarity, 44 (84.62%) cells reversed their migratory direction towards the right (Fig. 4C, grey, the mean directedness value was 0.596 ± 0.096), where the new cathode was located.

Directional cell migration is voltage dependent with a low threshold. To test the likelihood of a role for the endogenous EFs in directing cell migration, we determined migration of tracheobronchial epithelial cells in applied EFs at various strengths (0, 23, 48, and 90 mV/mm, respectively). To ensure comparability, data shown in Fig. 4 were from experiments that were done on the same day with cells from the same animal. The assay duration of each voltage strength lasted 90–100 min. Only the first 90 min were quantified. Migration directionality was quantified using the directedness value. Cells migrating in a random direction give a mean directedness value close to zero, as exemplified in control cells with no EF stimulation (0.035 ± 0.071). Application of an EF as small as 23 mV/mm (the lowest field strength tested) induced robust cathode-di-
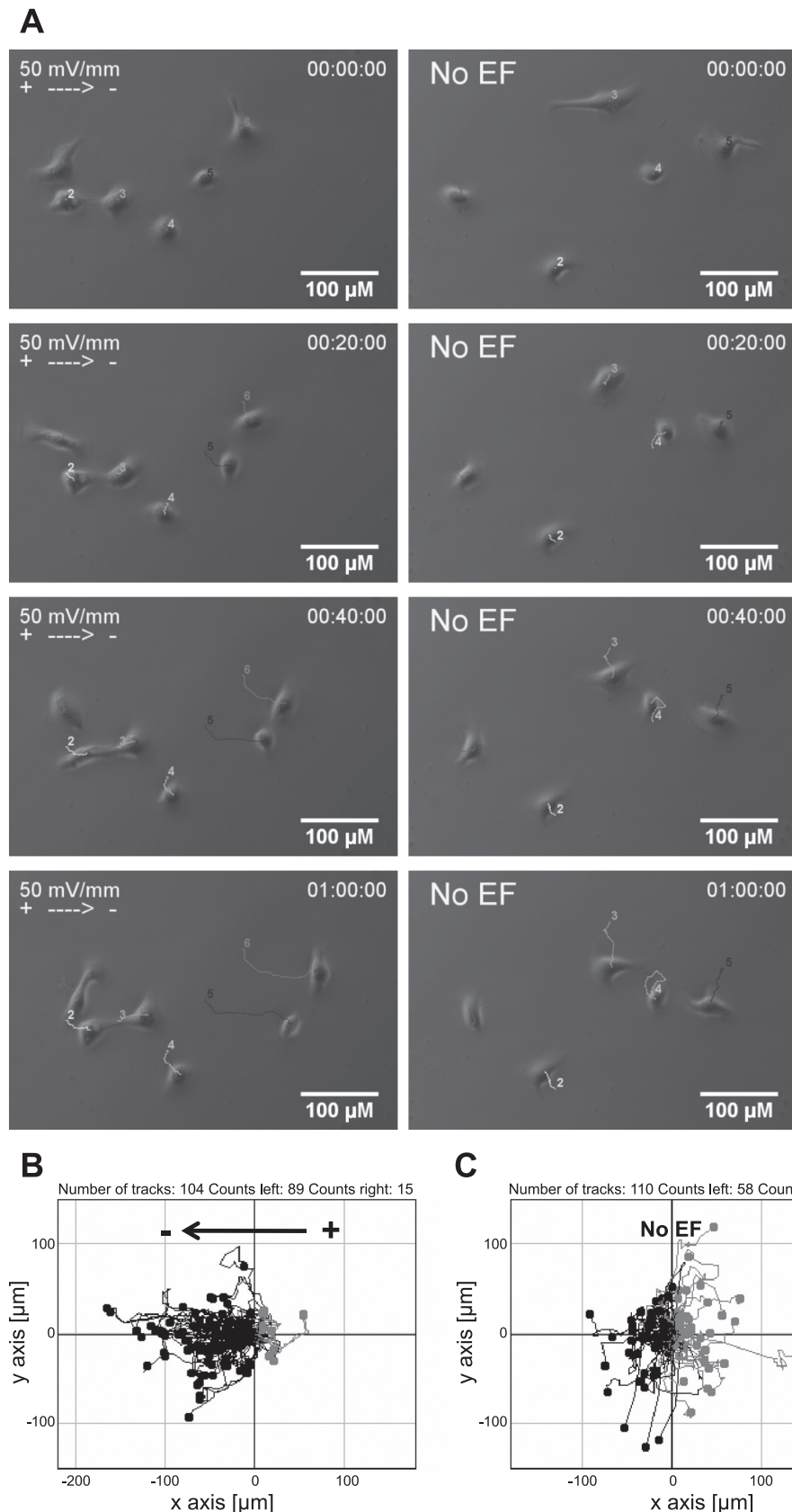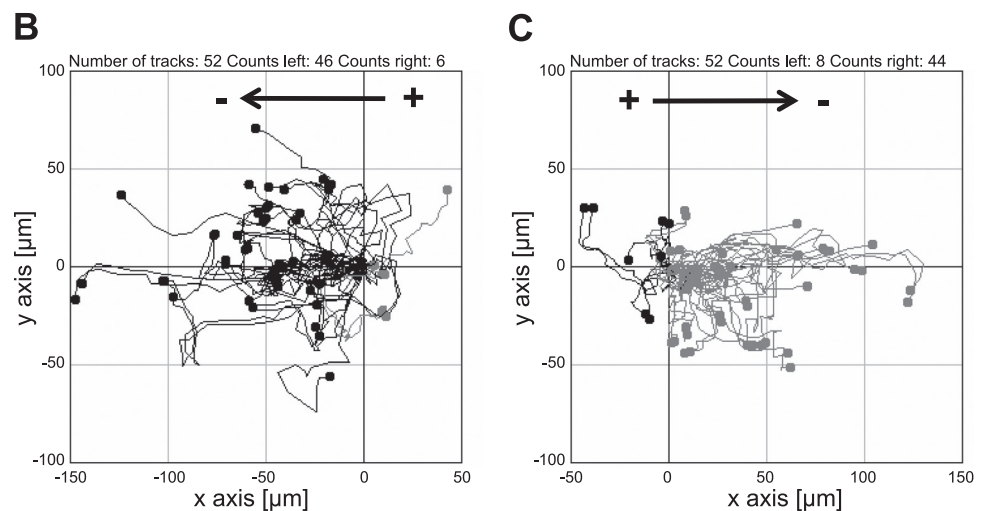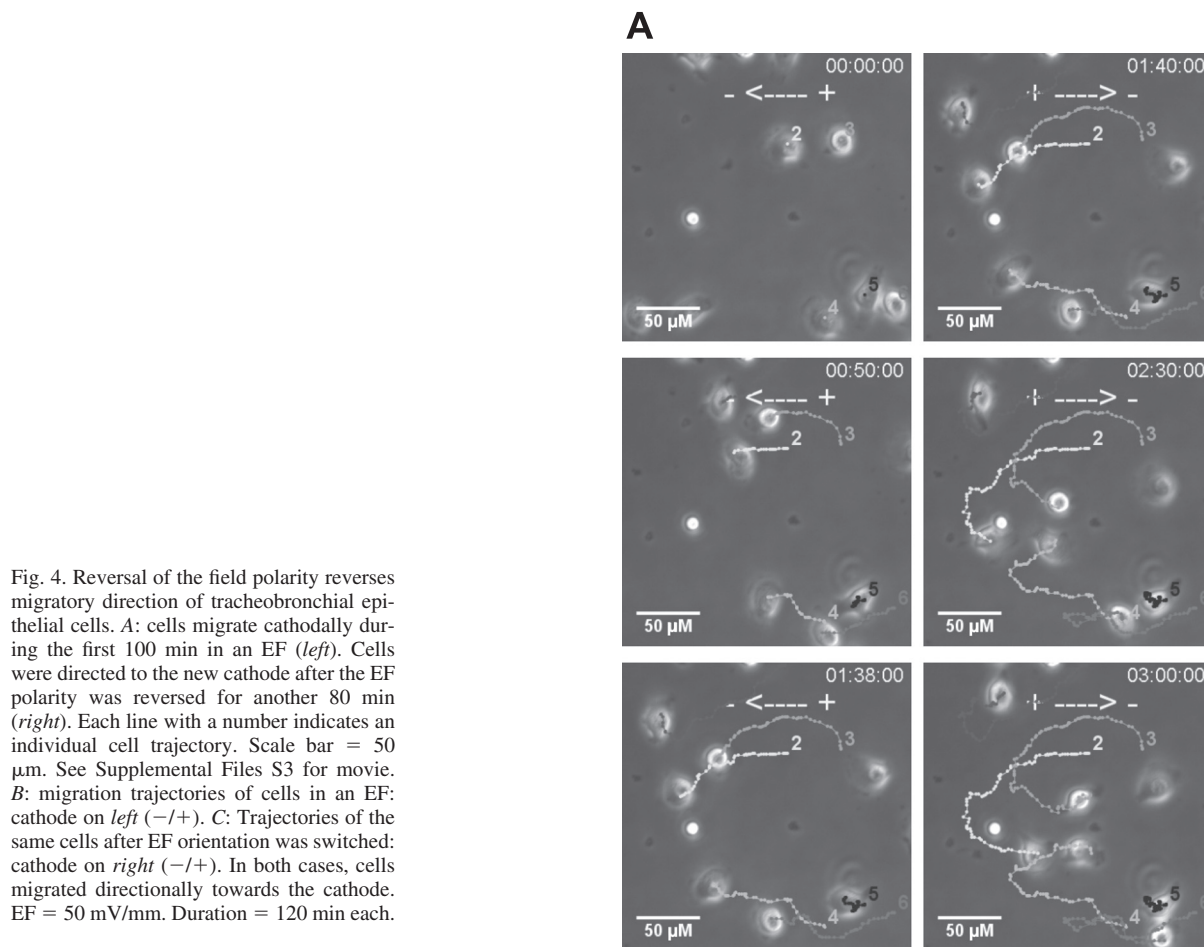
A

Fig. 3. Direct current electrical field (EF) direct migration of tracheobronchial epithelial cells of rhesus monkey towards the cathode. *A*: cell movement in an EF of 50 mV/mm was recorded with time-lapse microscopy (*left*). Cells migrate randomly in control conditions without an EF (*right*). Each line with a number indicates an individual cell trajectory. Scale bar = 100 μm. *B–C*: migration trajectories. Each dot represents an individual cell with its trajectory plotted in a Cartesian coordinate system, in which the start point of each cell is set as the origin. Cells that migrate towards the right are highlighted in gray. In an EF cells migrate cathodally to the left (*B*), compared with the control (no EF) in which cells migrate randomly (*C*). EF = 50 mV/mm. Duration = 145 min. See Supplemental Files S1 and S2 for movies.

B   **C**

A

Fig. 4. Reversal of the field polarity reverses migratory direction of tracheobronchial epithelial cells. *A*: cells migrate cathodally during the first 100 min in an EF (*left*). Cells were directed to the new cathode after the EF polarity was reversed for another 80 min (*right*). Each line with a number indicates an individual cell trajectory. Scale bar = 50 μm. See Supplemental Files S3 for movie. *B*: migration trajectories of cells in an EF: cathode on *left* (−/+). *C*: Trajectories of the same cells after EF orientation was switched: cathode on *right* (−/+). In both cases, cells migrated directionally towards the cathode. EF = 50 mV/mm. Duration = 120 min each.

B

C

rected migration of tracheobronchial epithelial cells with a directedness of 0.519 ± 0.091, significantly higher than that of control cells with no EF exposure ($P = 0.00047$). Further increasing EF strength to 48 mV/mm produced a higher directedness value of 0.701 ± 0.057. An additional significant increase in directedness (0.866 ± 0.044) was found when EF strength reached 90 mV/mm (Fig. 5*A*). At 90 mV/mm, many cultured cells migrated straight towards the cathode. We also tested an EF of 200 mV/mm in a single experiment. The

directionality reaches a maximum when cells are exposed to this EF strength (data not shown).

The effects on the migration speed, however, were not very consistent. The tracheobronchial epithelial cells of the no EF control, moved consistently with an average speed of 0.742 μm/min. Applying an EF of 23 mV/mm increased trajectory velocity to 0.896 ± 0.023 μm/min ($P = 0.014$ compared with the no EF control). However, in an EF of 48 mV/mm, the increase in the trajectory velocity (0.779 ± 0.021 μm/min) was
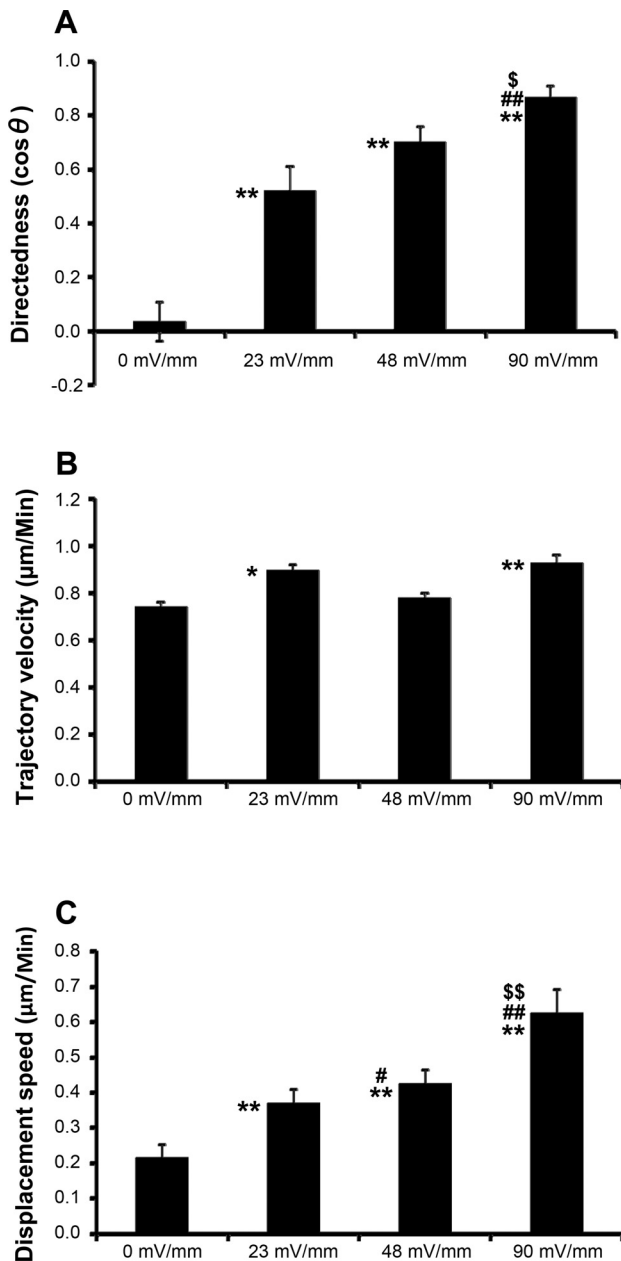
A

B

C

Fig. 5. Directional migration of rhesus monkey tracheobronchial epithelial cells is voltage dependent. *A*: directedness of cell migration (cosθ; θ is the angle between a straight line drawn from the cells start point to end point and the horizontal axis). *B*: trajectory velocity and *C*: displacement speed of cell migration were calculated as described in MATERIALS AND METHODS. Increasing voltage from 23 to 90 mV/mm enhanced directional migration. Duration of each tested voltage strength was 90 min. **$P < 0.01$, compared with no EF. ##$P < 0.01$, compared with EF of 23 mV/mm. #$P < 0.05$, compared with EF of 23 mV/mm. $$$P < 0.01$, compared with EF of 48 mV/mm. $$P < 0.05$, compared with EF of 48 mV/mm.

not significant, compared with that of either no EF control ($P = 0.491$) or an EF of 23 mV/mm ($P = 0.456$). In an EF of 90 mV/mm, cells moved faster (0.928 ± 0.034 μm/min, $P = 0.009$, compared with no EF control, Fig. 5*B*). Although the directedness cannot increase further, increasing the field strength to 200 mV/mm increased cell migratory speed dramatically (data not shown).

Application of EFs increased the efficiency of cell migration towards the cathode. Displacement speed represents how efficiently a cell migrates (the higher the speed, the more efficient the migration). Applying an EF (23, 48, or 90 mV/mm) caused tracheobronchial epithelial cells to migrate more efficiently (0.369 ± 0.039, 0.425 ± 0.039, 0.626 ± 0.067 μm/min, respectively) than the control cells with no EF exposure (0.215 ± 0.037 μm/min, Fig. 5*C*); these results are significant ($P = 8.2 \times 10^{-5}$, 7.8×10^{-9}, and 8.7×10^{-11}, respectively). Taken together, the improved efficiency of cathode-directed cell migration can be attributed to the enhancement of directionality, which is voltage dependent.

EFs promote tracheobronchial epithelial wound healing in vitro. Since applied EFs directed tracheobronchial epithelial cell migration in vitro, it is also reasonable to expect that the EF may promote wound healing through enhanced cell migration towards the wound. To test this idea, we used a wound healing assay, an extensively validated in vitro model to mimic cell migration in vivo (42). We applied external EFs across scratch "wounds" created with a standard 200-μl pipette tip in confluent monolayers of cultured tracheobronchial epithelial cells. For demonstration purposes, we used a voltage of 200 mV/mm, which is higher than that used to guide single cell migration. However, compared with cells under no EF conditions, even at this field strength no distinguishable morphological changes or signs of stress were observed during the 5-h course of time-lapse recording. As shown in Fig. 6*B*, applying an exogenous EF markedly enhanced tracheobronchial epithelial wound healing. Figure 6*B* shows time-lapse photomicrographs taken before (*top*) and 5 h after (*bottom*) electrical stimulation with strength and orientation as indicated. Control time-lapse photomicrographs without EF exposure are shown in Fig. 6*A*. Two parameters were used to quantify the wound healing efficiency. Figure 6*C* shows the dynamic change in remaining wound area from pooled data. Figure 6*D* shows the average speed of wound edge pushing towards the wound center. Only the wound edge facing the cathode was measured as the other side was withdrawn away from the wound center during application of the EF (Fig. 6*B*). The striking difference in tracheobronchial epithelial wound healing as a consequence of EF-enforced directed cell migration is highly significant (in both quantitative analyses, $P < 0.001$; $n = 4$). A movie consisting of the entire series of time-lapse photomicrographs from a representative experiment can be viewed (Supplemental Files S4 and S5).

DISCUSSION

Naturally occurring EFs at airway epithelial wounds. Respiratory epithelia transport ions and maintain a TEP (24, 39, 58). Whether wound EFs exist at airway epithelium, however, has not yet been tested. Using a vibrating probe to measure electric current, we showed that injury to airway epithelium resulted in endogenous wound electric currents in rhesus monkey trachea, with an outward current peaking at 1.6 μA/cm². These electric currents are similar to those found at mouse skin wounds and rat cornea wounds (13, 39). The measurements might be an underestimate due to ex vivo conditions.

The intact epithelium maintains an inward current through ion transport. A wound short circuits the TEP at the wound site, producing an outward current flow (Fig. 1*B*). The current flow
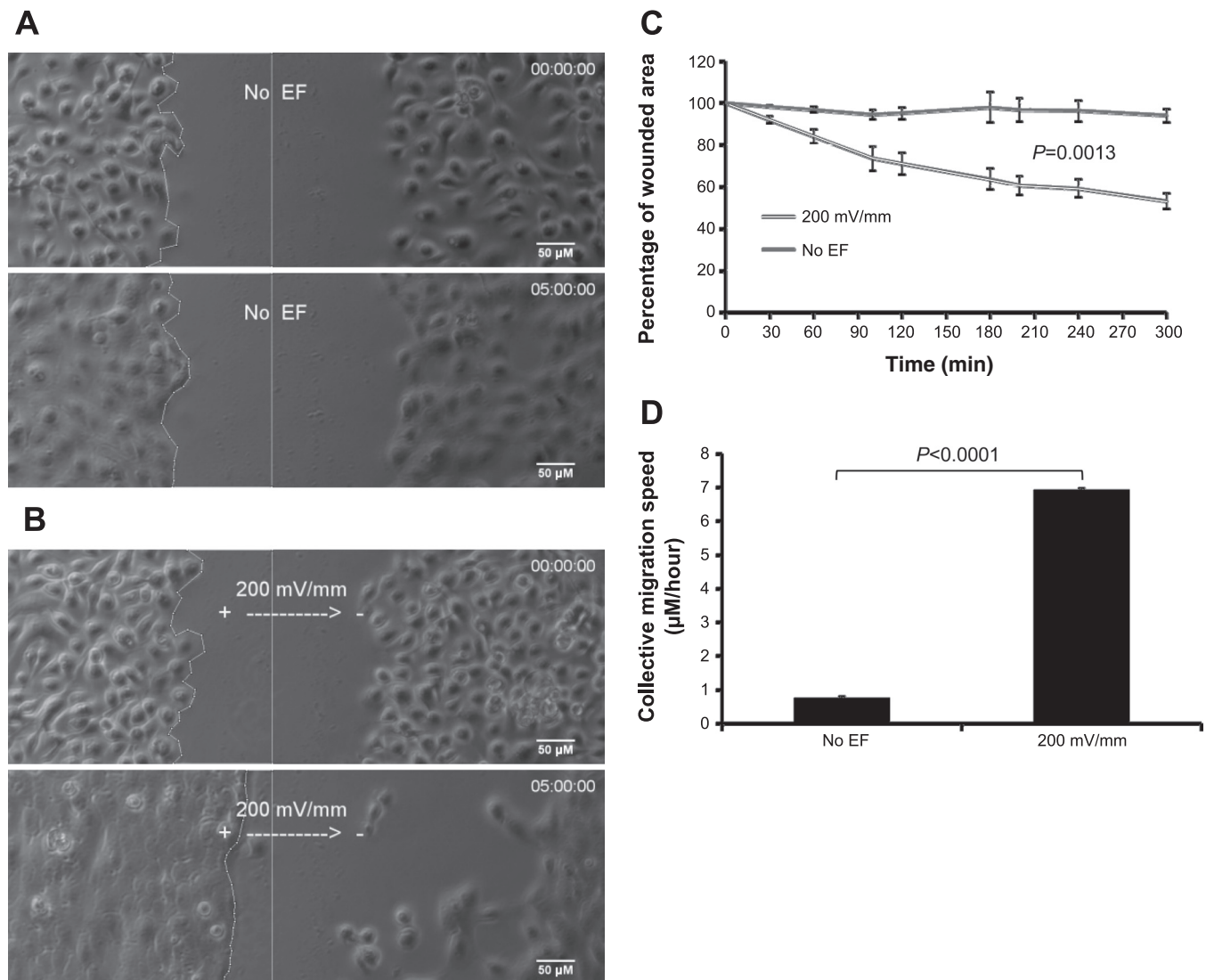
Fig. 6. EFs promote wound healing of cultured tracheobronchial epithelial cells. Cultured primary tracheobronchial epithelial cells were seeded in custom-made electrotactic chambers to form a monolayer. Scratch wounds were made using a standard 200-μl pipette tip. An EF of 200 mV/mm was applied across (perpendicular to) the scratch wounds. Wounds were monitored by time-lapse imaging for up to 5 h. *A*: beginning (*time 0*) and end photographs of no EF control. *B*: beginning (*time 0*) and end photographs of EF (200 mV/mm) exposure. Line on the *left* defines the wound edge. Straight line in the *middle* defines the center of the wound. Scale bars = 50 μm. See Supplemental Files S4 and S5 for movies. *C*: quantification of wound healing. Halves of the wound areas (line enclosed in *A* and *B*) at each time point were quantified and presented as a percentage of the original wound area. Difference between EF and no EF groups is significant ($P = 0.0013$; $n = 4$). *D*: wound edge migration speed: comparison between EF of 200 mV/mm and no EF control. Difference is significant ($P < 0.0001$; $n = 4$).

must form a complete loop, so an equal and opposite current must flow within the epithelium and underlying tissues to generate an intra-tissue field with the negative pole at the wound site, similar to skin and corneal wounds (39).

Addition of the ion transport enhancer aminophylline significantly increased the outward wound currents, indicating that ion channels are mechanistically involved in the airway epithelial wound, as previously found in wounded cornea (39). The electric currents at the tracheal wound decreased drastically in the presence of CFTR(Inh)-172, suggesting an important role for the apically localized CFTR (see *Directional migration of tracheobronchial epithelial cells in applied EFs* for more discussion). The endogenous wound electric currents are therefore likely to be an active and regulated response to injury.

Directional migration of tracheobronchial epithelial cells in applied EFs. Wound EFs offer a suitable cue to guide tracheobronchial epithelial cells in repairing wounds. An early step in wound healing involves migration of epithelial cells towards the site of injury. Tracheobronchial epithelial cells from rhesus monkeys respond to small EFs by migrating towards the cathode: the direction of the endogenous electric currents at the wound edge, towards the wound center. The threshold field strength required to induce significant directional migration is <23 mV/mm. The enhancement of directionality correlated well with the field strength (Fig. 5*A*). This response is similar to that seen in human keratinocytes and corneal epithelial cells (28, 60). Applied EFs appeared to increase the migratory speed, especially when the strength was high. The direction of migration and the threshold field strength, therefore, support

the hypothesis that the endogenous wound EFs serve as a guidance cue that directs epithelial cell migration to promote airway epithelial wound healing. When exposed to applied EFs, the displacement speed increased significantly, indicating more efficient migration.

Although the directionality is voltage dependent, the driving force of cell motility (speed of cell migration) changes little when the applied EF is in the physiological range (0 to 100 mV/mm). The influential view on how cells respond to directional signals is provided by the "compass model" (55). According to this model, the motile machinery, coupled with the chemical reaction-diffusion system of phosphatidylinositol 3-kinase-kinase lipid products and Rho GTPases, exhibits the inherent ability to self-polarize. Without a persistent signal, a self-polarized cell moves with a characteristic speed, but with an inconsistent direction, which changes often and randomly. In the presence of a signal, in our case electrical, the "motile compass" is oriented: the cell direction aligns with the EF and fluctuates less, and the cell moves with more consistent directionality.

The majority of primary cultured monkey airway epithelial cells did not express cilia on their surface, especially after prolonged cultivation. This is likely due to the ciliated epithelial cells undergoing squamous metaplasia as observed in mice during the early stage of bronchiolar epithelial repair. In that model, squamous metaplasia of the ciliated cells occurred within 6–12 h after injury, spreading to cover the denuded area induced by naphthalene (33). It is traditionally believed that ciliated cells are terminally differentiated cells that are not able to divide (37). The nonciliated cells, which displayed the ability to directionally migrate in an applied EF, might be (or be originally derived from) resident stem/progenitor cells (for example Clara cells), which are abundantly distributed throughout the airway epithelium (8).

Recent studies have uncovered many aspects of the repair processes that follow airway epithelial injury. These consist of complex multistages in which a cascade of multicellular interactions and tissue remodeling must proceed in an orderly fashion for optimal functional recovery. The initial phase, characterized by epithelial cells migrating to cover denuded areas, is followed by proliferation to replace injured cells, and differentiation to establish squamous or mucous cell metaplasia. Consequently, more epithelial cells are present after proliferation, so some of the cells must be discarded to restore the epithelium to the original condition. Soon after the cell numbers have been reduced to those found in unexposed individuals, the normal proportions of cell types are restored (36). It has been proposed that these repair processes may be orchestrated and regulated by local production of proinflammatory cytokines, chemotactic signals, and growth factors (2). In the present work, we provide the first experimental evidence clearly showing that application of EFs normally present in injured airway epithelium accelerates wound healing. In the in vivo situation, airway epithelial wound healing may be enhanced by endogenous electric stimulation in many different ways. The one implicated by the present study suggests that electric potentials have the capacity to directly guide cell migration as supported by our in vitro single cell migration data. Although this is hard to test at this time due to the difficulties in accessing and applying EFs in vivo, it is likely that an electric potential gradient (negative in the wound center) builds up at the site of injury, providing a guidance cue to migratory epithelial cells in surrounding intact tissue. One could imagine that this endogenous potential gradient must change dynamically in both strength and orientation so that the injured site can be covered efficiently and promptly. The endogenous EFs also affect cell proliferation and differentiation, which may contribute to wound healing (25, 58). These biological processes are just as important as cell migration and are likely to happen in later stages, which were excluded from our experiments as our observation time was limited to 5 h (Fig. 6). We emphasize that the biophysical electric signal will not be the only signal necessary for airway epithelial repair. Other mechanisms such as biochemical cues play equally important roles and are likely to interact with each other. Damaged epithelial cells and other cell types release cytokines and growth factors that regulate cellular processes such as chemotaxis, cell proliferation, angiogenesis, extracellular matrix production, and remodeling. Although the molecular mechanisms involved in these early major steps of the repair process are largely unknown, failed or delayed recovery of airway epithelial damage increases chances for opportunistic infection resulting from breached mucosal barrier function, resulting in the permanent changes observed in diseases such as asthma, chronic obstructive pulmonary disease, and acute respiratory distress syndrome. Therefore, elucidating the origin of the endogenous electric potential and how it is regulated may provide ideas for novel therapies.

CFTR, airway epithelial wound-associated electric potential, and their potential roles in wound healing. CFTR is the major Cl^- channel in the apical membranes of many secretary epithelia, including airway epithelium, and is activated by intracellular cAMP (10). The significant enhancement of outward current by aminophylline, as measured from wounded tracheal epithelium, indicates the important role of ion transport in generating wound electric currents. CFTR appears to be one of the main elements responsible for the ionic transport, because addition of CFTR(Inh)-172, a specific CFTR inhibitor, significantly reduced the wound-associated electric current (Fig. 2). It would be very interesting to test whether airway epithelial injury or damage induces CFTR expression, or changes its biosynthesis process in the remaining epithelial cells, or the cells adjacent to the wound.

Pharmacological drugs which alter ion transport (and subsequently wound EFs) affect wound healing rate in rat cornea (39). The thiazolidinone compound CFTR(Inh)-172 reversibly and selectively inhibits CFTR Cl^- conductance with high potency and minimal cellular toxicity (23). Our preliminary data suggest that inhibition of CFTR by complete blockage of CFTR Cl^- conductance significantly delays wound closure in cultured tracheal epithelial cell monolayer (personal communication, Y.-H. Sun and M. Zhao). This result is consistent with a recent study, revealing that wound healing in cystic fibrosis was significantly delayed (up to 33%) compared with normal, non-cystic fibrosis controls (51). Moreover, during the preparation of this manuscript, another group conducted independent experiments to investigate the role of CFTR in airway epithelial cell migration and wound closure using normal human bronchial epithelial cells and a human airway epithelial cell line (Calu-3) of serous gland origin (43). As well as CFTR(Inh)-172, they used CFTR-specific shRNA to silence CFTR transcription, and found that inhibition of CFTR delayed airway epithelial wound closure significantly.

Interestingly, these authors found that loss of CFTR transport activity restricts lamellipodia (the "steering device" for cells in motion) protrusion at cell leading edges. Collectively, these data suggest that mechanisms of airway epithelial wound healing may involve endogenous EFs, and that these EFs may depend on the functioning of CFTR, and it is likely that other selective ion channels are involved also.

In summary, we have detected a steady electric potential arising from wounded airway epithelium in a nonhuman primate model. Small applied EFs provide a powerful guidance cue to direct migration of tracheobronchial epithelial cells and promote wound healing. Ion channels, especially CFTR, appear to play a significant role in regulating this injury-associated electric current. Pharmacological manipulation of ion transport in airway epithelium may offer a new approach to improve airway epithelial repair.

DISCLOSURES

No conflicts of interest, financial or otherwise, are declared by the author(s).

REFERENCES

1. **Avdalovic MV, Putney LF, Schelegle ES, Miller L, Usachenko JL, Tyler NK, Plopper CG, Gershwin LJ, Hyde DM.** Vascular remodeling is airway generation-specific in a primate model of chronic asthma. *Am J Respir Crit Care Med* 174: 1069–1076, 2006.
2. **Bennett NT, Schultz GS.** Growth factors and wound healing: biochemical properties of growth factors and their receptors. *Am J Surg* 165: 728–737, 1993.
3. **Borgens RB.** Endogenous ionic currents traverse intact and damaged bone. *Science* 225: 478–482, 1984.
4. **Borgens RB, Jaffe LF, Cohen MJ.** Large and persistent electrical currents enter the transected lamprey spinal cord. *Proc Natl Acad Sci USA* 77: 1209–1213, 1980.
5. **Chiang M, Robinson KR, Vanable JW Jr.** Electrical fields in the vicinity of epithelial wounds in the isolated bovine eye. *Exp Eye Res* 54: 999–1003, 1992.
6. **Crawford I, Maloney PC, Zeitlin PL, Guggino WB, Hyde SC, Turley H, Gatter KC, Harris A, Higgins CF.** Immunocytochemical localization of the cystic fibrosis gene product CFTR. *Proc Natl Acad Sci USA* 88: 9262–9266, 1991.
7. **Crosby LM, Waters CM.** Epithelial repair mechanisms in the lung. *Am J Physiol Lung Cell Mol Physiol* 298: L715–L731, 2010.
8. **Crystal RG, Randell SH, Engelhardt JF, Voynow J, Sunday ME.** Airway epithelial cells: current concepts and challenges. *Proc Am Thorac Soc* 5: 772–777, 2008.
9. **Fulcher ML, Gabriel SE, Olsen JC, Tatreau JR, Gentzsch M, Livanos E, Saavedra MT, Salmon P, Randell SH.** Novel human bronchial epithelial cell lines for cystic fibrosis research. *Am J Physiol Lung Cell Mol Physiol* 296: L82–L91, 2009.
10. **Fuller CM, Benos DJ.** CFTR!. *Am J Physiol Cell Physiol* 263: C267–C286, 1992.
11. **Godfrey RW.** Human airway epithelial tight junctions. *Microsc Res Tech* 38: 488–499, 1997.
12. **Gruler H, Nuccitelli R.** Neural crest cell galvanotaxis: new data and a novel approach to the analysis of both galvanotaxis and chemotaxis. *Cell Motil Cytoskeleton* 19: 121–133, 1991.
13. **Guo A, Song B, Reid B, Gu Y, Forrester JV, Jahoda CA, Zhao M.** Effects of physiological electric fields on migration of human dermal fibroblasts. *J Invest Dermatol* 130: 2320–2327, 2010.
14. **Holgate ST.** The airway epithelium is central to the pathogenesis of asthma. *Allergol Int* 57: 1–10, 2008.
15. **Holgate ST.** Pathogenesis of asthma. *Clin Exp Allergy* 38: 872–897, 2008.
16. **Horwitz B.** Electrophoretic migration due to postsynaptic potential gradients: theory and application to autonomic ganglion neurons and to dendritic spines. *Neuroscience* 12: 887–905, 1984.
17. **Huttenlocher A, Horwitz AR.** Wound healing with electric potential. *N Engl J Med* 356: 303–304, 2007.
18. **Jaffe LF, Nuccitelli R.** An ultrasensitive vibrating probe for measuring steady extracellular currents. *J Cell Biol* 63: 614–628, 1974.
19. **Knight DA, Holgate ST.** The airway epithelium: structural and functional properties in health and disease. *Respirology* 8: 432–446, 2003.
20. **Levin M.** Large-scale biophysics: ion flows and regeneration. *Trends Cell Biol* 17: 261–270, 2007.
21. **Liu X, Luo M, Zhang L, Ding W, Yan Z, Engelhardt JF.** Bioelectric properties of chloride channels in human, pig, ferret, and mouse airway epithelia. *Am J Respir Cell Mol Biol* 36: 313–323, 2007.
22. **Lucas R, Verin AD, Black SM, Catravas JD.** Regulators of endothelial and epithelial barrier integrity and function in acute lung injury. *Biochem Pharmacol* 77: 1763–1772, 2009.
23. **Ma T, Thiagarajah JR, Yang H, Sonawane ND, Folli C, Galietta LJ, Verkman AS.** Thiazolidinone CFTR inhibitor identified by high-throughput screening blocks cholera toxin-induced intestinal fluid secretion. *J Clin Invest* 110: 1651–1658, 2002.
24. **McCaig CD, Rajnicek AM, Song B, Zhao M.** Controlling cell behavior electrically: current views and future potential. *Physiol Rev* 85: 943–978, 2005.
25. **McCaig CD, Song B, Rajnicek AM.** Electrical dimensions in cell science. *J Cell Sci* 122: 4267–4276, 2009.
26. **Mukerjee EV, Isseroff RR, Nuccitelli R, Collins SD, Smith RL.** Microneedle array for measuring wound generated electric fields. *Conf Proc IEEE Eng Med Biol Soc* 1: 4326–4328, 2006.
27. **Nadel JA, Davis B, Phipps RJ.** Control of mucus secretion and ion transport in airways. *Annu Rev Physiol* 41: 369–381, 1979.
28. **Nishimura KY, Isseroff RR, Nuccitelli R.** Human keratinocytes migrate to the negative pole in direct current electric fields comparable to those measured in mammalian wounds. *J Cell Sci* 109: 199–207, 1996.
29. **Nuccitelli R.** Endogenous electric fields in embryos during development, regeneration and wound healing. *Radiat Prot Dosimetry* 106: 375–383, 2003.
30. **Nuccitelli R.** A role for endogenous electric fields in wound healing. *Curr Top Dev Biol* 58: 1–26, 2003.
31. **Nuccitelli R, Nuccitelli P, Ramlatchan S, Sanger R, Smith PJ.** Imaging the electric field associated with mouse and human skin wounds. *Wound Repair Regen* 16: 432–441, 2008.
32. **Ojingwa JC, Isseroff RR.** Electrical stimulation of wound healing. *J Invest Dermatol* 121: 1–12, 2003.
33. **Park KS, Wells JM, Zorn AM, Wert SE, Laubach VE, Fernandez LG, Whitsett JA.** Transdifferentiation of ciliated cells during repair of the respiratory epithelium. *Am J Respir Cell Mol Biol* 34: 151–157, 2006.
34. **Plopper CG, Heidsiek JG, Weir AJ, George JA, Hyde DM.** Tracheobronchial epithelium in the adult rhesus monkey: a quantitative histochemical and ultrastructural study. *Am J Anat* 184: 31–40, 1989.
35. **Plopper CG, Hyde DM.** The non-human primate as a model for studying COPD and asthma. *Pulm Pharmacol Ther* 21: 755–766, 2008.
36. **Puchelle E, Zahm JM, Tournier JM, Coraux C.** Airway epithelial repair, regeneration, and remodeling after injury in chronic obstructive pulmonary disease. *Proc Am Thorac Soc* 3: 726–733, 2006.
37. **Rawlins EL, Hogan BL.** Ciliated epithelial cell lifespan in the mouse trachea and lung. *Am J Physiol Lung Cell Mol Physiol* 295: L231–L234, 2008.
38. **Reid B, Nuccitelli R, Zhao M.** Non-invasive measurement of bioelectric currents with a vibrating probe. *Nat Protoc* 2: 661–669, 2007.
39. **Reid B, Song B, McCaig CD, Zhao M.** Wound healing in rat cornea: the role of electric currents. *FASEB J* 19: 379–386, 2005.
40. **Riordan JR.** CFTR function and prospects for therapy. *Annu Rev Biochem* 77: 701–726, 2008.

41. **Robinson KR, Messerli MA.** Left/right, up/down: the role of endogenous electrical fields as directional signals in development, repair and invasion. *Bioessays* 25: 759–766, 2003.
42. **Rodriguez LG, Wu X, Guan JL.** Wound-healing assay. *Methods Mol Biol* 294: 23–29, 2005.
43. **Schiller KR, Maniak PJ, O'Grady SM.** Cystic fibrosis transmembrane conductance regulator is involved in airway epithelial wound repair. *Am J Physiol Cell Physiol* 299: C912–C921, 2010.
44. **Sheridan DM, Isseroff RR, Nuccitelli R.** Imposition of a physiologic DC electric field alters the migratory response of human keratinocytes on extracellular matrix molecules. *J Invest Dermatol* 106: 642–646, 1996.
45. **Song B, Gu Y, Pu J, Reid B, Zhao Z, Zhao M.** Application of direct current electric fields to cells and tissues in vitro and modulation of wound electric field in vivo. *Nat Protoc* 2: 1479–1489, 2007.
46. **Song B, Zhao M, Forrester JV, McCaig CD.** Electrical cues regulate the orientation and frequency of cell division and the rate of wound healing in vivo. *Proc Natl Acad Sci USA* 99: 13577–13582, 2002.
47. **Stripp BR, Reynolds SD.** Maintenance and repair of the bronchiolar epithelium. *Proc Am Thorac Soc* 5: 328–333, 2008.
48. **Sumi Y, Hamid Q.** Airway remodeling in asthma. *Allergol Int* 56: 341–348, 2007.
49. **Tai G, Reid B, Cao L, Zhao M.** Electrotaxis and wound healing: experimental methods to study electric fields as a directional signal for cell migration. *Methods Mol Biol* 571: 77–97, 2009.
50. **Tomkiewicz RP, Albers GM, De Sanctis GT, Ramirez OE, King M, Rubin BK.** Species differences in the physical and transport properties of airway secretions. *Can J Physiol Pharmacol* 73: 165–171, 1995.
51. **Trinh NT, Prive A, Maille E, Noel J, Brochiero E.** EGF and K^+ channel activity control normal and cystic fibrosis bronchial epithelia repair. *Am J Physiol Lung Cell Mol Physiol* 295: L866–L880, 2008.
52. **Vieira AC, Reid B, Cao L, Mannis MJ, Schwab IR, Zhao M.** Ionic components of electric current at rat corneal wounds. *PLos One* 6: e17411, 2011.
53. **Wang E, Zhao M, Forrester JV, McCaig CD.** Bi-directional migration of lens epithelial cells in a physiological electrical field. *Exp Eye Res* 76: 29–37, 2003.
54. **Ware LB, Matthay MA.** The acute respiratory distress syndrome. *N Engl J Med* 342: 1334–1349, 2000.
55. **Weiner OD.** Regulation of cell polarity during eukaryotic chemotaxis: the chemotactic compass. *Curr Opin Cell Biol* 14: 196–202, 2002.
56. **Zadunaisky JA, Lande MA, Chalfie M, Neufeld AH.** Ion pumps in the cornea and their stimulation by epinephrine and cyclic-AMP. *Exp Eye Res* 15: 577–584, 1973.
57. **Zahm JM, Pierrot D, Chevillard M, Puchelle E.** Dynamics of cell movement during the wound repair of human surface respiratory epithelium. *Biorheology* 29: 459–465, 1992.
58. **Zhao M.** Electrical fields in wound healing–an overriding signal that directs cell migration. *Semin Cell Dev Biol* 20: 674–682, 2009.
59. **Zhao M, Agius-Fernandez A, Forrester JV, McCaig CD.** Directed migration of corneal epithelial sheets in physiological electric fields. *Invest Ophthalmol Vis Sci* 37: 2548–2558, 1996.
60. **Zhao M, Agius-Fernandez A, Forrester JV, McCaig CD.** Orientation and directed migration of cultured corneal epithelial cells in small electric fields are serum dependent. *J Cell Sci* 109: 1405–1414, 1996.
61. **Zhao M, Song B, Pu J, Wada T, Reid B, Tai G, Wang F, Guo A, Walczysko P, Gu Y, Sasaki T, Suzuki A, Forrester JV, Bourne HR, Devreotes PN, McCaig CD, Penninger JM.** Electrical signals control wound healing through phosphatidylinositol-3-OH kinase-gamma and PTEN. *Nature* 442: 457–460, 2006.